PII: S0955-2219(98)00157-5

0955-2219/98/$—see front matter

Boundary Stress and its Effect on Toughness in Thin Boundary Layered and Particulate Composites: Model Analysis and Experimental Test on Y-TZP-based Ceramic Composites

J. L. Shi,* L. Li and J. K. Guo

State Key Laboratory of High Performance Ceramics and Superfine Microstructure, Shanghai Institute of Ceramics, 1295 Ding-Xi Road, Shanghai, 200050, People's Republic of China

(Received 20 March 1998; revised version received 14 June 1998; accepted 16 June 1998)

Abstract

The average thermal residual stress in continuous boundary phase of polycrystalline ceramic composites was calculated with a simple thin boundary layer model and a criterion for the self-cracking of the boundary phase was derived under a certain assumption. From the proposed model, the toughness of the materials can be increased by both tensile and compressive stress at boundaries when the crack propagates transgranularly; and will be increased when the stress at boundary is compressive for intergranular fracture mode. The maximum increase is predicted to be achieved at the boundary phase content not higher than 33%. The experimental results with Y-TZP doped with different kinds of grain boundary phase show a qualitative agreement with the prediction by the model but the toughness increase is largely dependent on the distribution feature of glass phases. From the ideal particle-in-infinite matrix model, the average stress in matrix and in particle for possible practical system was estimated and compared with the thin boundary layer model. The criterion for the self-cracking in matrix and in particle or at the particle–matrix interface was derived with stress intensity factor approach. From the existing periodic stress field model for particulate composite, the toughness increase is found not to increase monotonously with the content of second phase. Alternatively a maximum toughness increase is found, which is predicted to be achieved at the particulate phase content of 14·3 vol%. The experimental results on Y-TZP/Al_2O_3 composites were compared with the prediction of the model.

*To whom correspondence should be addressed.

1 Introduction

During cooling down of ceramics from sintering temperature, the size of grains decreases by the rate of its expansion (or more accurately, shrinkage) coefficients. However, as recognized widely by the material researchers, the residual stress at grain boundary and between different phases is generated if there is a difference of the shrinkage rates between grains and/or between phases. The residual stress by the different shrinkage rates has been calculated using very simplified model, e.g. one particle in infinite uniform matrix model.[1] Recently the residual stress distribution for some more complicated systems was calculated based on the ideal particle-in-infinite matrix model.[2] The estimation of stress and the effect of residual stress on the toughness of the composites has been made for particulate dispersed composites.

Toughness increase of the various composite materials, including particulate composites,[3–6] whisker[7–9] and fiber[10,11] reinforced material systems has been observed intensively. The toughness increase has been attributed to several mechanisms such as crack bowing,[12] crack deflections[9,13,14] bridging and pull-out[9,11] of whiskers, fibers or elongated grains behind the crack tip, and so on. Estimation of the contribution of various mechanisms to the toughening effect of the composites was also attempted.[5,9,11] However, most of these effects is, as a matter of fact, associated with the boundary stress.[2] For example, the crack deflection is caused by the stress field around a second phase particle for particulate composites; and the toughening effect partially caused by the friction force acted on fiber or whiskers for fiber and/or whisker reinforced

composites is also the results of the residual stress. Moreover, in spite of this, the contribution of these mechanisms like crack deflection to the toughness increase does not account to the total increase for the toughness of particulate reinforced composites.[15,16] It has been recognized that there will be an effect of the residual stress itself on the mechanical properties,[15] as being estimated quantitatively by Taya *et al.*,[16] that the periodic stress field[15] in the particulate composites does contribute to the toughness increase. Some work on WC–Co hard alloy[17,18] has been conducted with the concept of periodic stress field, which shows the dependence of the toughness of the materials on the size of WC particles based on particle dispersion model.

In addition to the particulate composites, which are generally fabricated by solid state sintering at relatively high temperatures or by hot-pressing, composites with thin continuous or semi-continuous grain boundary glass phase can be fabricated simply by pressureless sintering at relative low temperature. Therefore this kind of materials is of significance in practice. The mechanical properties of the polycrystalline ceramics with continuous or semi-continuous grain boundary phase are shown to be usually good enough for practical application, but nevertheless are subjected to the properties and distribution of the grain boundary phase. The theoretical description of the continuous or semi-continuous boundary stress and its effect on the properties of ceramics were not be found in literature. Considering the possible differences in the thermal properties between the ceramic matrix and grain boundary phase, it is believed that the effect of such difference on crack propagation and therefore fracture toughness of ceramic composites should also exist. The present paper is to calculate the boundary stress aroused by the difference in thermal properties and analyze the critical conditions for the self cracking of the boundary phase and the contribution of the thermal residual stress to the toughness of materials studied. The experimental results on Y-TZP (yttria stabilized tetragonal zirconia polycrystals) based materials with glass boundary phase will be presented afterwards. The particulate composites (particle dispersed system) were also analyzed for effect of residual stress on the toughness increase. In this case Y-TZP/Al_2O_3 system was tested.

2 Experimental Procedure

Y-TZP material was selected as the matrix for composites with continuous or semi-continuous grain boundary phase. The superfine Y-TZP powder was prepared via coprecipitation method. The details of the preparation method can be found in previous published work.[19] Three kinds of Al_2O_3–SiO_2 based glass phase were selected: Li_2O–Al_2O_3–SiO_2, MgO–Al_2O_3–SiO_2 and Na_2O–Al_2O_3–SiO_2. The detailed chemical compositions and thermal expansion coefficients of materials are listed in Tables 1 and 2. The glass components were mixed together with the Y-TZP powder by ball milling for 8 h with agate balls and the content of the glass phases was designed to be 0, 1, 2 and 5 vol%.

The above material systems were selected for the thin boundary layer model as proposed below. For particulate composite the typical oxide particle/particle system was Y-TZP/Al_2O_3. Composite materials were fabricated both by mechanical mixing of nano-Y-TZP powder with alumina powders and by coprecipitation of mixed solution of Zr^{4+}, Y^{3+} and Al^{3+}. The details of the fabrication procedure of the composites can be found in the previous reports.[20–22]

The Y-TZP/Glass and Y-TZP/Al_2O_3 composite materials were sintered at 1250 and 1550°C for 2 h, respectively, and the densities were measured with the Archimedes method in distilled water. Fracture toughness was measured by SENB (single edge notched beam) method with a notch width of 0·2 mm and a span of 20 mm, or Vicker's indentation method according to the equation proposed by Shetty *et al.*[23] for the indentation-induced Palmqvist crack system.

3 Model Analysis

3.1 Thin grain boundary model

3.1.1 Model assumption

If the content of the grain boundary phase is not high enough as compared with the matrix and the interface energy between glass phase and the matrix grains is low enough as compared with that

Table 1. Compositions (wt%) for the three kinds of glass

	SiO_2	Al_2O_3	Li_2O	MgO	Na_2O	TiO_2	$\alpha\times10^{-6}$
LAS	72·5	21·0	6·50				< 1
MAS	58·2	19·2		13·4		9·2	6·3
NAS	44·5	31·5			16·7	7·3	11·4

Table 2. The percentage (ΔK_{Ic}%) of the fracture toughness increase of the Y-TZP/glass composites and the difference ($\Delta\alpha$) of the thermal expansion coefficients of glass phase with Y-TZP ($\alpha_{Y\text{-}TZP}=11\times10^{-6}\ K^{-1}$)

	Y-TZP/LAS			*Y-TZP/MAS*			*Y/TZP/NAS*		
$\Delta\alpha\times10^{-6}\ K^{-1}$	> 10			4·7			0·4		
C_{glass}%	1	2	5	1	2	5	1	2	5
ΔK_{Ic}%	42	32	24	22	18	13	8	2	−2

between matrix grains, boundary phase can spread uniformly at all boundaries throughout the material. Then glass phase can be treated as a thin layer with an identical thickness, t, between matrix grains, as is shown schematically in Fig. 1. If thickness t is small as compared with the grain size of D, to simplify the problem, the residual stress within the layer is assumed to be uniform and the stress in matrix grains is also treated as an average value.

3.1.2 Calculation of the residual stress

The thermal residual stress formed during cooling down from the sintering temperature can be calculated according to the strain difference between the practical strain in the composites and the strain in single phase materials from the stress relaxation temperature of each material to room temperature. For the plane stress condition of mode I, the stresses could be expressed as:

$$\sigma_b = E_b(\langle\varepsilon\rangle - \varepsilon_b) \tag{1}$$

$$\sigma_m = E_m(\langle\varepsilon\rangle - \varepsilon_m) \tag{2}$$

where $\langle\varepsilon\rangle$ is the practical true strain, and this strain is assumed to be uniform within the composite body, ε_b, ε_m are the respective strains for the grain boundary phase and the matrix phase when not restrained by each other from the relaxation temperature to room temperature, σ_b and σ_m are the stresses in boundary and in matrix; E_b and E_m are the Young's modulus of grain boundary and matrix phases, respectively.

According to the balance condition for material in unconstrained condition,

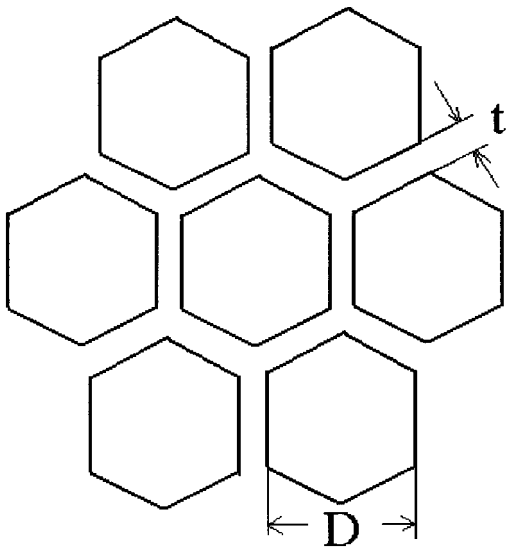

Fig. 1. Schematic drawing for the thin boundary layer model, where t is the thickness of the boundary and D represents the particle size.

$$C_b\sigma_b + (1 - C_b)\sigma_m = 0 \tag{3}$$

where C_b is the content of the boundary phase, and the value of strain, $\varepsilon_b = \langle\alpha_b\rangle\Delta T$, $E_m = \langle\alpha_m\rangle\Delta T$, here $\langle\alpha_b\rangle$ and $\langle\alpha_m\rangle$ are the average value of the thermal expansion coefficients for boundary and matrix phases. The average strain can be calculated as follows:

$$\langle\varepsilon\rangle = \frac{E_b\alpha_b C_b + E_m\alpha_m(1 - C_b)}{E_b C_b + E_m(1 - C_b)} \cdot \Delta T = \langle\alpha\rangle\Delta T \tag{4}$$

therefore the thermal residual stress in boundary and in matrix grain can be calculated as follows:

$$\sigma_b = E_b(\langle\alpha\rangle - \alpha_b)\Delta T \tag{5}$$

$$\sigma_m = E_m(\langle\alpha\rangle - \alpha_m)\Delta T \tag{6}$$

here $\langle\alpha\rangle$ is the average thermal expansion of the composite. According to the thermal behavior of the composites, $\langle\alpha\rangle$ can be calculated from the data of $\langle\alpha_m\rangle$ and $\langle\alpha_b\rangle$ and eqn (4).

From the above calculation, it can be found that when $\alpha_m > \alpha_b$, (i.e. $\langle\alpha\rangle > \alpha_b$), $\sigma_b < 0$, the grain boundary will be in compression and the matrix will be in tension; and if $\alpha_m < \alpha_b$, ($\langle\alpha\rangle < \alpha_b$), $\sigma_m < 0$, in contrast the grain boundary will be in tension and the matrix will be in compression on average.

3.1.3 The allowable maximum residual stress for the self-cracking of the materials

The thermal residual stress may cause self-cracking if the tensile stress is overlarge. Under the condition of compressive stress in boundary, the tensile stress in matrix is supposed to be very small and the self-cracking of matrix is believed to be negligible. When the boundary is in tension, the tensile stress may cause cracking in boundary. The critical boundary stress would be:

$$\sigma_c = E_b(\langle\alpha\rangle - \alpha_b)\Delta T = yK_{IC}C^{1/2} \tag{7}$$

here K_{IC} is the toughness of the boundary phase, C is the half critical defect length and y is a geometric constant. Regarding the value of C being proportional to the matrix particle size, D, there will be:

$$\sigma_c^2 D = \text{constant} \tag{8}$$

3.1.4 Effect of the boundary stress on the toughness of the composites

a. For the intergranular cracking mode

When cracks propagate along the grain boundaries, the cracking resistance will be affected by the

stress in the boundary. If the boundary is under the stress of σ_b, there will be the strain energy at the boundary, the energy density (strain energy per unit of boundary area) will be:

$$d_e = 1/2\varepsilon_b\sigma_b t\left(\mathrm{J\ m^{-2}}\right) \tag{9}$$

where t is the thickness of the boundary. The cracking along the boundary is associated with the release of the strain energy. Let χ be the release ratio of the strain energy in boundary (the strain energy in matrix is considered not released during the cracking of boundary), the cracking (fracture) energy will be:

$$\gamma_{f,b} = \gamma^0_{f,b} \pm 1/2\chi\varepsilon_b\sigma_b t \tag{10}$$

where $\gamma_{f,b}$ and $\gamma^0_{f,b}$ are the fracture energy of the boundary with and without the thermal residual stress, respectively. Considering the simple relation between the thickness of boundary, t, and the grain size, D for cubic shaped grains: $t = C_b D/3$, under the plane stress condition for mode I, there will be:

$$\begin{aligned} K_{1c} &= [2\gamma_{f,b}E_b]^{1/2} \\ &= [2E_b\gamma^o_{f,b} \pm \chi\sigma_b^2 DC_b/3]^{1/2} \\ &= [(K^o_{1c})^2 \pm \chi\sigma_b^2 DC_b/3)]^{1/2} \end{aligned} \tag{11}$$

From the above equation, the condition for self-cracking can also be derived when the boundary is under tension:

$$D\sigma^2 < 6\gamma^o_{f,b}E_b/\chi C_b = 3\left(K^o_{1c}\right)^2/\chi E_b C_b \tag{12}$$

b. For the transgranular cracking mode

For this type of crack propagation mode, the crack travel through a periodic field of stress, i.e. the crack propagates stepwisely through a compressive–tensile stress field. The schematic drawing for the stress field through which a crack propagate is presented in Fig. 2. Under the cracking mode, where the stress field exerts an resistance to the crack propagation, the resistance can be expressed as an additional stress intensity factor acting on the crack tip, K^R_I:[18]

$$K^R_I = \frac{1}{(\pi a)^{1/2}}\int_{-a}^{a}\sigma(x)\left(\frac{a+x}{a-x}\right)^{1/2}\mathrm{d}x \tag{13}$$

where a is the period of the stress field, x is a point within the period, $\sigma(x)$ is the function of x. The result of this integration is dependent on the stress

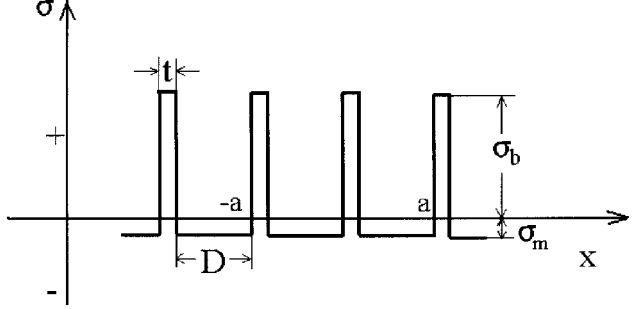

(a)

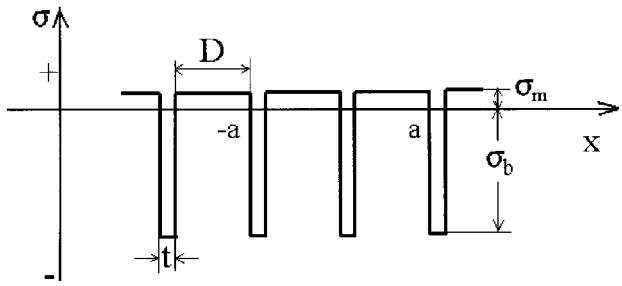

(b)

Fig. 2. Periodic stress field in the proposed model system presented at Fig. 1: (a) $\alpha_b > \alpha_m$, (b) $\alpha_b < \alpha_m$.

state of the boundary. For $\alpha_m < \alpha_b$, matrix is under compression:

$$K^R_I = -A_1\sigma_m D^{1/2} \tag{14}$$

and for $\alpha_m > \alpha_b$, boundary is under compression:

$$K^R_I = -A_2\sigma_b t^2 \tag{15}$$

where A_1 and A_2 are constants. So it is clear that only the compressive stress would be effective in altering the additional stress intensity factor. For the crack propagating in the stress field, total critical stress intensity factor will be:

$$K^a_I + K^R_I \geq K^o_{1c} \tag{16}$$

here K^a_I is the applied critical stress intensity factor, K^o_{1c} is the toughness of the materials without the stress field, and this applied critical stress intensity factor is, as a matter of fact, the toughness of the material:

$$K_{10} = K^o_{1c} + A_1\sigma_m D^{1/2} \quad (\text{when } \alpha_m < \alpha_b) \tag{17}$$

and

$$K_{1c} = K^o_{1c} + A_2\sigma_b t^{1/2} \quad (\text{when } \alpha_m > \alpha_b) \tag{18}$$

3.2 Particle dispersion model for particulate composites

3.2.1 Average stress estimation

3.2.1.1. Average stress estimation based on ideal model. Stress field for a spherical particle-in-uniform matrix has been known for a long time.[1] When the radius of matrix, R_o approaches infinity, the stress (P_o) in particle is:

$$P_o = -\frac{(\alpha_p - \alpha_m)}{\frac{1+\nu_m}{2E_m} + \frac{1-2\nu_p}{E_p}} \Delta T \tag{19}$$

The stress in the matrix $\sigma_r = P_o\left(\frac{R}{r}\right)^3$ for the radial stress, and $\sigma_\theta = -\frac{1}{2}\sigma_r$ for circumferential stress, where R is the radius of the particle, and r is the distance from a point in matrix to the particle's center.

a. $\infty > R_o \gg R$: under the condition the average stress in the particle is assumed to be unchanged, but that in matrix can be estimated as follows:

$$\begin{aligned}\langle\sigma_r\rangle &= -P_o \int_R^{R_o} \left(\frac{R}{r}\right)^3 4\pi r^2 \, \mathrm{d}r \frac{1}{\frac{4\pi}{3}\left(R_o^3 - R^3\right)} \\ &= P_o \frac{3R^3}{R_o^3 - R^3} \ln\frac{R_o}{R} \\ &\approx 3P_o\left(\frac{R}{R_o}\right)^3 \ln\frac{R_o}{R}\end{aligned}$$

$$\langle\sigma_\theta\rangle = P_o\left(\frac{R}{R_o}\right)^3 \ln\frac{R_o}{R} \tag{21}$$

b. $R_o > R$, and $(R_o - R)/R \sim 1$: in this case the calculation will be very complicated. A simplified calculation for average stress, $\langle\sigma_m\rangle$, is presented as follows:

Let the stress in particle $P = \alpha P_o$, $0 < \alpha < 1$, to associate the value of α with the volume percentage of particle, C_p, let $\alpha = f(C_p)$, we have:

$$P = f(C_p) P_o \tag{22}$$

According to the balance principle: $(1 - C_p)\langle\sigma_m\rangle + PC_p = 0$

$$\langle\sigma_m\rangle = -\frac{P_o f(C_p) C_p}{1 - C_p} = -\frac{P_o f(C_p) R^3}{R_o^3 - R^3} \tag{23}$$

c. $R_o > R$ and $R_o/R \to 1$: according to eqn (23), when the matrix (a thin layer in this case) around the spherical particle is thin enough, the following relation is present:

$$\langle\sigma_m\rangle = -\frac{P_o f(C_p) C_p}{(1 - C_p)} = -\frac{P_o f(C_p) D}{6t} \tag{24}$$

here D is the diameter of the spherical particle and t is the thickness of the layer. Simply let $f(C_p) = 1 - C_p$, eqns (23) and (24) become:

$$P = (1 - C_p) P_o \quad \text{and} \quad \langle\sigma_m\rangle \approx -C_p P_o \tag{25}$$

3.2.1.2. Estimation of the average stress in practical system. As reported by Taya *et al.*,[16] the average stress in particulate composite system can be estimated to be:

$$\langle\sigma_p\rangle = -\frac{2E_p(1 - C_p)\beta\varepsilon_p}{A} \tag{26}$$

$$\langle\sigma_m\rangle = \frac{2E_m C_p \beta\varepsilon_p}{A} \tag{27}$$

here β and A are the constant associated with the material parameter:

$$\begin{aligned}\beta &= \left[(1 + \nu_m)/(1 - 2\nu_p)\right](E_p/E_m) \\ A &= (1 - C_p)(\beta + 2)(1 + \nu_m) + 3\beta C_p(1 - \nu_m)\end{aligned} \tag{28}$$

and ε_p is the misfit strain of particle:

$$\varepsilon_p = \int_{T_L}^{T_R} (\alpha_p - \alpha_m)\delta \, \mathrm{d}T \tag{29}$$

where T_R and T_L are the room temperature and the temperature at which the stress is totally relaxed, δ is the isotropic tensor (Kronechner's delta).

3.2.2 Critical particle size estimation

3.2.2.1. Critical particle size estimation for the self-cracking in matrix when $\alpha_m > \alpha_p$. The critical particle size for the spontaneous cracking of particulate composites has been estimated by Lange[24] with the energy balance approach. Green[25] also discussed the problem and proposed a general relation with the stress intensity factor approach:

$$D_c^{\min} \propto (K_c/E\varepsilon)^2 \tag{30}$$

for the particulate composite by assuming that the properties of the second phase are the same as the matrix, i.e. regarding the composite as a 'single phase' material, here $D_c^{\min}$ is the critical grain size, ε is the linear residual.[25]

Generally the mechanical properties of particulate phase is different from the matrix phase. In the

case of $\alpha_m > \alpha_p$, the matrix is possible to crack initialized from the particle-matrix interface under the tensile circumferential stress aroused by the thermal expansion mismatch and a penny-shaped crack may form around the spherical particle. Therefore the second phase particle in matrix can be regarded as the source of cracking, i.e. the defect of the critical size, from which matrix could crack. According to the Griffth equation for critical materials, we have:

$$D_{oc} = B(K_{1c}/y\sigma_{\theta\max})^2 = B'(K_{1c}/P)^2 \qquad (31)$$

where K_{1c} is the toughness of matrix, B and B' are constants.

It is not attempted to calculate the constant B and D_{oc}, as the calculated values are usually much smaller than those in practice.[25] Equations (8), (12) and (31) are in agreement with each other in nature and also with that proposed by Lange[24] and Green.[25] If the particle matches well with the matrix, e.g. the difference of the thermal expansion coefficients is close to each other, the critical particle size will be large enough and the possibility for self-cracking will be small.

For the particles of non-spherical shape, the above criterion is believed to be applicable qualitatively in principle.

3.2.2.2. Critical particle size estimation for the self-cracking when $\alpha_m < \alpha_p$. If the particle is in tension and the matrix is in compression, there will be the possibility for the cracking in particle or at the particle–matrix interface. Simply from the viewpoint of stress intensity factor, regarding the dimension of particle diameter particle as being proportional to defect size, the critical particle size can be calculated as:

$$D_{oc} \propto \left(K_{1c,p}/yP\right)^2 \qquad (32)$$

for cracking in particle, where $K_{1c,p}$ is the fracture toughness of particle, $K_{1c,p} = \left(2E_p\gamma_{f,p}\right)^{1/2}$, $\gamma_{f,p}$ is the fracture energy of particle, P is the tensile stress within the particle, and

$$D_{oc} \propto (K_{1c,i}/yP)^2 \qquad (33)$$

for cracking at the particle–matrix interface, where $K_{1c,i}$ is the critical stress intensity factor at the particle–matrix interface, $K_{1c,i} = (2E_i\gamma_{f,i})^{1/2}$, E_i is the average Young's modulus and $\gamma_{f,i}$ is the fracture energy at the interface.

3.2.3 Effect of the residual stress on the fracture toughness

In the practical particulate composites, crack propagates through the periodic stress field in which the tensile and compressive stress alternates with an approximately constant period. With the model shown in Fig. 2 which is formerly proposed by Culter,[18] the relation between the toughness of the particle dispersed composite and the residual stress field would be:[18]

$$K_{1c} = K^o_{1c} - K^R_I = K^o_{1d} + A_3\sigma_m(Q_m)^{1/2} \qquad (34)$$

for the condition $\alpha_m < \alpha_p$, the matrix is under compression, here A_3 is a constant, σ_m is the compressive stress and Q_m is the periodic length of compressive stress in matrix, and

$$K^c_I = K^o_{1c} - K^R_I = K^o_{1c} + A_4\sigma_p\left(Q_p\right)^{1/2} \qquad (35)$$

when $\alpha_m > \alpha_p$, the particle is under compression, here A_4 is another constant, σ_p is the compressive stress and Q_p is the periodic length of the compressive stress in particle.

4 Experimental Results and Discussions

4.1 Thin boundary layer model: mechanical properties of Y-TZP/glass composites

Figure 3 gives the relative density of the materials sintered at 1250°C. The results show that the single phase Y-TZP can be sintered to 94·4% of the theoretical density, and higher sintered density of the composites can be achieved when the glass phase is added. Glass phase is present at the boundaries and/or at the triple points among the Y-TZP grains, as can be seen in Fig. 4.

Figure 5 gives the toughness of the composite measured by Vicker's indentation method using the formula proposed by Shetty, *et al.*[23] The toughness of pure Y-TZP as determined by SENB (single edge notched beam) method with the sample dimension of 2·5×5×25, span of 20 mm and notch width of 0·2 mm. The results of SENB method are

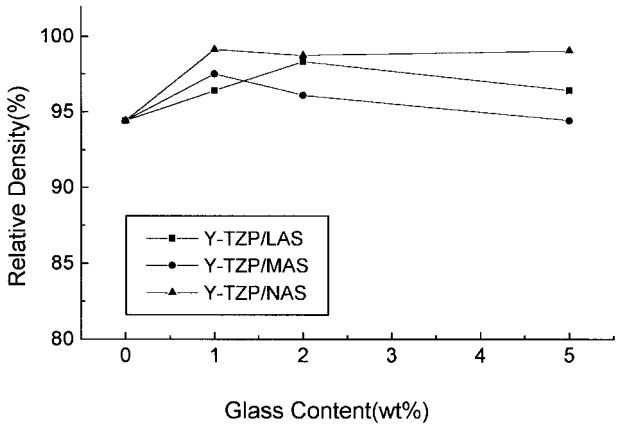

Fig. 3. Relative density of the Y-TZP/glass composites sintered at 1250°C for 2 h.

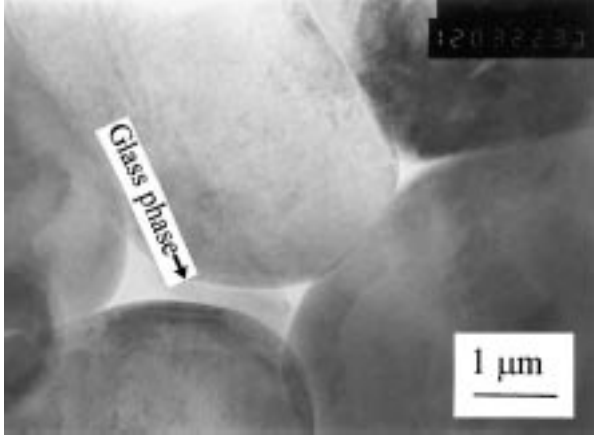

Fig. 4. TEM microstructure of Y-TZP/LAS-glass with the glass content of 2 vol%.

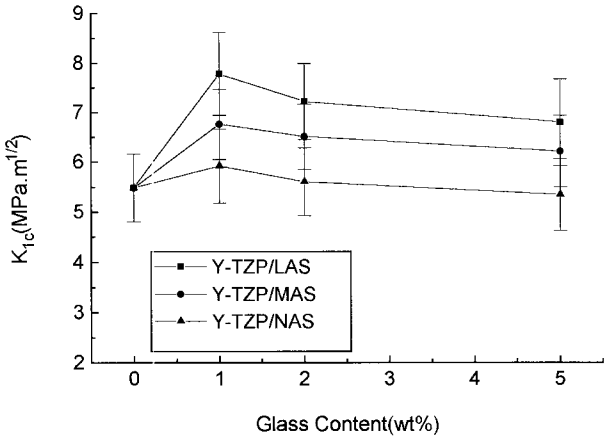

Fig. 5. Fracture toughness of the Y-TZP/glass composites as a function of the glass phase content.

higher than that by the indentation method. Results show clearly that when small amount of glass phase is added, the toughness of the composite changes and the percentage of the change is shown in Table 2. The percentage of the change of the composites follows the order of LAS > MAS > NAS. This order can be related to the difference of the thermal expansion coefficients of the glass phase with Y-TZP (see Table 2).

4.2 Relation between K_{1c} and the content of the boundary phase

The fracture mode of Y-TZP and Y-TZP/glass composite is basically intergranular. According to eqn (11), the toughness of the composite will increase if the boundary is in compression. As a matter of factor, the glass phase used in this study is indeed in compression according to the equation, and toughness does increase in the order of the difference of the thermal expansion coefficients. However the relation between the toughness and the glass phase content in practice is largely different from the prediction by the model, as analyzed as follows.

4.2.1 For the intergranular mode

From eqns (4) and (5), K_{1c} of the composites can be found to increase with the content of the boundary phase first and then decrease. The content at which maximum K_{1c} can be achieved, $C_{b,m}$, as the first approximation and when $\alpha_b < \alpha_m$, is as follows:

$$C_{b,m} = \frac{\alpha_m - \alpha_b}{3\left(\alpha_m - \frac{E_b}{E_m}\alpha_b\right)} \tag{36}$$

It can be seen that $C_{b,m}$ would be equal to 33% when $E_b \approx E_m$. However, the experimental results show that the $C_{b,m}$ value is much lower that 33%. This discrepancy can be explained with the different distribution characteristics of the glass phase at different contents of glass and the different value of γ_f^0. At low glass content, the glass phase tend to accumulate at the triple points, and then crack propagates through the interface between Y-TZP grains, so the value of γ_f^0 is, as a matter of fact, very close to that of Y-TZP ceramics, $\gamma_{f,TZP}^0$. At higher glass content when the glass phase can spread uniformly and form a continuous or semi-continuous thin layer at the boundaries, the fracture energy would be that of boundary phase or between Y-TZP grain and the boundary phase, i.e. the values of γ_f^0 is that of glass boundary phase, $\gamma_{f,b}^0$, or that of between Y-TZP matrix and glass, $\gamma_{f,b-m}^0$. As commonly known the boundary phase is glass, $\gamma_{f-g}^0 \ll \gamma_{f,TZP}^0$, and $\gamma_{f,b-m}^0$ is also believed to be much less than $\gamma_{f,TZP}^0$, therefore according to eqn (11) only at very low content of glass phase the toughness increase can be obtained. With the increase of glass phase contribution, the toughness of the composites will decrease due to the decreasing interface energy.

4.2.2 For the transgranular mode

For this kind of fracture mode, from eqns (4) and (18), the value of $C_{b,m}$ is the same as shown in eqn (36). However, the transgranular mode in Y-TZP/glass composite was not found.

4.3 Particulate composites: mechanical properties of Y-TZP/Al_2O_3 composites

Figure 6 gives the results of fracture toughness of mechanically mixed Y-TZP/Al_2O_3 composites measured by both SENB method and Vicker's indentation methods. The results show that the composite toughness increases with alumina content and the maximum occurs at 5 vol%. Another set of data for the similar materials system but with different processing (coprecipitation) method shows the very similar results, as can be found in Fig. 7. Part of the toughness increase can be attributed to the phase transformation volume as reported previously,[25] however, the effect of thermal residual stress is not negligible.

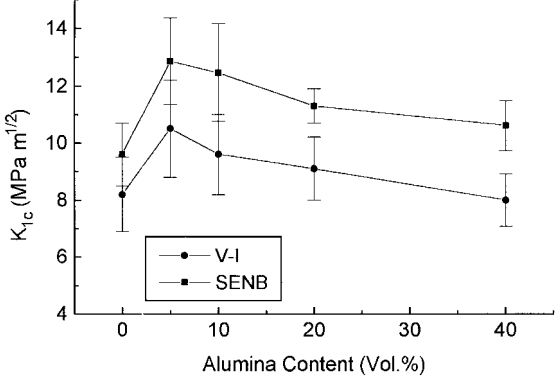

Fig. 6. Fracture toughness of mechanically mixed Y-TZP/Al_2O_3 composites as a function of alumina content, (■) by single edge notched beam method, (●) by Vickers indentation method.

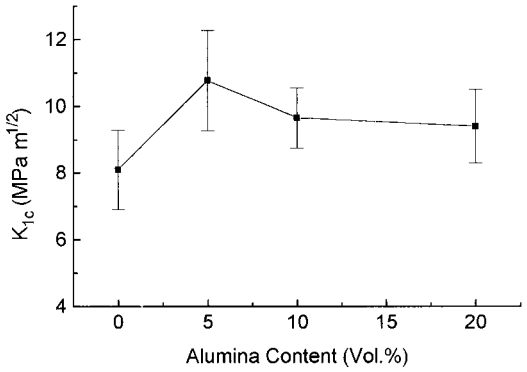

Fig. 7. Fracture toughness of coprecipitated Y-TZP/Al_2O_3 composites as a function of alumina content by Vicker's indentation method.

4.4 Relation between K_{1c} and the content of particulate phase

The analysis by former researchers[14,16] shows that the toughness of the composite increases monotonously with the increase of the particulate phase content. This conclusion is usually not the case in practice. The practical results often show that there is a maximum toughness increase at a certain content of particulate phase. This content can be estimated from the proposed model in Fig. 2. From eqn (25) or (26), and eqn (35), the toughness increase by the particulate phase is:

$$\Delta K_{1c} = A\sigma_p (Q_p)^{1/2} \propto (1 - C_p)(Q_p)^{1/2} \qquad (37)$$

It can be found from eqn (37) that there will be a maximum increase of toughness at a given content of particulate phase. Let Q_p be proportional to the particle diameter, and assuming that the particle number is unchanged when the content changes, a simple calculation show that the given content of the particulate phase for maximum toughness increase is 14·3 vol%. This estimation has been proven to be qualitatively applicable for the reports by many researchers for various particulate composite systems in literature, such as for Y-TZP/TiC_p, Al_2O_3/SiC_p, Al_2O_3/Y-TZP_p, and so on.[4–6,26] The experimental data by Taya[16] are too few to show this phenomena and his model did not give this rule. Other models[7,14] based on the crack deflection or whisker or grain pullout did not predict this rule either. The practical content of particular phase for the maximum toughness for the present system is lower than that value, which is thought to be caused by the feature of phase transformation during fracture, as the phase transformation volume is shown to be larger at smaller particulate phase content.

5 Conclusion

1. A thin boundary layer model is presented and the boundary stress for composites with glass phase is calculated. the stress occurred to be dependent on the thermal expansion and the content of the boundary phase. The criterion for self-cracking at boundary is estimated and shown to be dependent on the toughness of boundary and the stress level.
2. Toughness of the composite material is predicted from the proposed model to increase for both tensile and compressive stress at boundaries when the crack propagates transgranularly. For intergranular fracture mode toughness will increase when the stress at boundary is compressive.
3. The experiment results with Y-TZP/glass composite show a qualitative agreement with the prediction given by the model but the glass content for the toughness maximum is much lower than predicted. This fact is explained by the different fracture energy at different glass content.
4. Average stress in possible particulate composite system was estimated and compared with the thin boundary layer model. The criterion for the self-cracking in matrix or in particle or at the particle–matrix interface was put forward with the stress intensity factor approach by regarding the particle as the defect of critical size.
5. From the periodic stress field model for particulate composites it is found that at 14·3 vol% of the particulate phase content, the toughness maximum for composites will be achieved. This result is different for the prediction made by several existing models.
6. The experimental results on Y-TZP/Al_2O_3 composites show the toughness increase of composites by adding alumina particles. The results obtained were compared with the prediction made for the periodic stress field model.

References

1. Selsing, J., Internal stress in ceramics. *J. Am. Ceram. Soc.*, 1961, **44**, 419.
2. Hong, Z. and Zongzhe, J., Analysis of residual stress and toughening mechanism for particulate composites. *J. Chin. Ceram. Soc.*, 1996, **24**(5), 491–497.
3. Budiansky, B., Amazigo, J. C. and Evans, A. G., Small-scale crack bridging and the fracture toughness of particulate-reinforced ceramics. *J. Mech. Phys. Solids*, 1988, **36**, 167–187.
4. Wei, G. C. and Becher, P. F., Improvements in mechanical properties in SiC by the addition of TiC particles. *J. Am. Ceram. Soc.*, 1984, **67**(8), 571–574.
5. Zhan, G. D., Lai, T. R., Shi, J. L. and Yen, T. S., Microstructure and mechanical properties of yttria-stabilized tetragonal zirconia polycrystals containing dispersed TiC particles. *J. Mater. Sci.*, 1996, **31**, 2903–2907.
6. Zhang, Y. F., Deng, Z. Y., Shi, J. L., Mao, Y. Q. and Guo, J. K., Microstructure and mechanical properties of SiC particle reinforced Al_2O_3 matrix composites. *J. Mater. Sci. Lett.*, 1996, **15**, 1927–1931.
7. Becher, P. F., Hsueh, C. H., Angelini, P. and Tiegs, T. N., Toughening behaviour in whisker-reinforced ceramic matrix composites. *J. Am. Ceram. Soc.*, 1988, **71**(12), 1050–1061.
8. Zhan, G. D., Shi, J. L., Zhou, Y., Zhan, Y. Z., Lai, T. R. and Yen, T. S., Fabrication, characterization and mechanical properties of SiC-whisker-reinforced Y-TZP composites. *J. Mater. Sci.*, 1996, **31**, 3237–3243.
9. Becher, P. F., Microstructural design of toughened ceramics. *J. Am. Ceram. Soc.*, 1991, **74**(2), 255–269.
10. Marshall, D. B. and Evans, A. G., Failure mechanism in ceramic–fiber–ceramic–matrix composites. *J. Am. Ceram. Soc.*, 1985, **68**(5), 225–231.
11. Evans, A. G., Perspective with development of high toughness ceramics. *J. Am. Ceram. Soc.*, 1990, **73**(2), 187–206.
12. Lange, F. F., The interaction of a crack front with a second-phase dispersion. *Philos. Mag.*, 1970, **22**, 983–992.
13. Evans, A. G., The strength of brittle materials containing second phase dispersion. *Philos. Mag.*, 1972, **26**, 1327–1344.
14. Faber, K. T. and Evans, A. G., Crack deflection process—I. Theory. *Acta Matell.*, 1983, **31**(4), 565–756.
15. Virkar, A. V. and Johnson, D. L., Fracture behaviour of ZrO_2–Zr composites. *J. Am. Ceram. Soc.*, 1977, **60**(11–12), 514–519.
16. Taya, M., Hayashi, S., Kobayashi, A. S. and Yoon, H. S., Toughening of a particulate-reinforced ceramic–matrix composite by thermal residual stress. *J. Am. Ceram. Soc.*, 1990, **73**(5), 1382–1391.
17. Chermant, J. L. and Ostersteck, F., Fracture toughness and fracture of WC–Co composites. *J. Mater. Soc.*, 1976, **1**, 1936–1951.
18. Culter, R. V. and Virkar, A. V., The effect of binder thickness and residual stress on the fracture toughness of cemented carbides. *J. Mater. Sci.*, 1985, **20**(12), 3557–3573.
19. Shi, J. L., Lin, Z. X. and Yen, T. S., Effect of agglomerates in superfine zirconia powder compacts on the microstructural development. *J. Mater. Sci.*, 1993, **28**, 342–348.
20. Shi, J. L. and Yen, T. S., Densification and microstructure development of alumina/Y-TZP composite powder (Y-TZP-rich) compacts. *Journal of the European Ceramic Society*, 1995, **15**(4), 363–369.
21. Shi, J. L., Li, B. S., Yuan, M. L. and Yen, T. S., Processing of nano-sized Al_2O_3/Y-TZP composite powders, I Preparation and characterization of the composite powders. *Journal of the European Ceramic Society*, 1995, **15**(10), 959–966.
22. Shi, J. L., Gao, J. H., Li, B. S. and Yen, T. S., Processing of nano-sized Al_2O_3/Y-TZP composite powders, II Densification and microstructure development. *Journal of the European Ceramic Society*, 1995, **15**(10), 967–974.
23. Shetty, D. K., Wright, I. G., Mincer, P. N. and Clauer, A. H., Indentation fracture of WC–Co cermets. *J. Mater. Sci.*, 1985, **20**, 1873–1882.
24. Lange, F. F., Criteria for crack extension and arrest in residual, localized stress fields associated with second phase particles. In *Fracture Mechanics of Ceramics*, Vol. 2, eds R. C. Bradt, D. P. H. Hasselman and F. F. Lange. Plenum Press, New York, 1974, pp. 599–609.
25. Green, D. J., Microcracking mechanism in ceramics, In *Fracture mechanics of Ceramics*, Vol. 5, ed. R. C. Bradt, A. G. Evans, D. P. H. Hasselman and F. F. Lange. Plenum, New York and London, 1983, pp. 457–478.
26. Shi, J. L. and Yen, T. S., Mechanical properties of Al_2O_3/Y-TZP composites and its toughening mechanism. *J. Mater. Sci.*, 1993, **28**(15), 4019–4022.